RESEARCH ARTICLE | SEPTEMBER 24 2025

High-pressure elasticity and equation of state of the fluoroelastomer Viton® A-500

Charlie M. Zoller ; Jonathan Simon; Rostislav Hrubiak ; Curtis Kenney-Benson ; Stephen A. Gramsch ; Dana M. Dattelbaum ; Muhtar Ahart ; Russell J. Hemley

AIP Advances 15, 095129 (2025)
https://doi.org/10.1063/5.0293539
CHORUS

High-pressure elasticity and equation of state of the fluoroelastomer Viton® A-500

Cite as: AIP Advances 15, 095129 (2025); doi: 10.1063/5.0293539
Submitted: 11 August 2025 • Accepted: 5 September 2025 •
Published Online: 24 September 2025

Charlie M. Zoller,[1,a] Jonathan Simon,[2] Rostislav Hrubiak,[3] Curtis Kenney-Benson,[3] Stephen A. Gramsch,[4] Dana M. Dattelbaum,[5] Muhtar Ahart,[1] and Russell J. Hemley[1,4,6]

AFFILIATIONS

[1] Department of Physics, University of Illinois Chicago, Chicago, Illinois 60607, USA
[2] Department of Mechanical and Industrial Engineering, University of Illinois Chicago, Chicago, Illinois 60607, USA
[3] HPCAT, Advanced Photon Source, Argonne National Laboratory, Lemont, Illinois 60334, USA
[4] Department of Chemistry, University of Illinois Chicago, Chicago, Illinois 60607, USA
[5] Dynamic Experiments Division, Los Alamos National Laboratory, Los Alamos, New Mexico 87545, USA
[6] Department of Earth and Environmental Sciences, University of Illinois Chicago, Chicago, Illinois 60607, USA

[a] **Author to whom correspondence should be addressed:** czoller2@uic.edu

ABSTRACT

Viton® A is a semi-crystalline copolymer of polyvinylidene fluoride and hexafluoropropylene used in various engineering applications due to its mechanical properties and chemical inertness. *In situ* ultrasonic spectroscopy and x-ray radiography measurements were performed in a Paris–Edinburgh press to measure the pressure dependence of the transverse and longitudinal acoustic velocity of the fluoroelastomer A-500 from 2.7 to 5.7 GPa at 296 K. In addition, we performed high-pressure Brillouin scattering measurements to obtain acoustic velocities from ambient pressure to 5.7 GPa to supplement the ultrasonic measurements, especially at low pressures. The acoustic velocities were then used to calculate a pressure–volume (P–V) equation of state, the bulk and shear moduli, and the Poisson's ratio. These quantities are compared with the reported pressure-dependent properties of related polymers over this range of pressures.

I. INTRODUCTION

Perfluorinated polymers have seen widespread use in engineering applications due to their mechanical properties, processability, and chemical inertness.[1] Viton® A-500 is a semi-crystalline copolymer of polyvinylidene fluoride (PVDF) and hexafluoropropylene (HFP).[2] PVDF has the chemical formula $CF_2 = CH_2$ and a glass transition temperature (T_g) of −40 °C, while HFP has the chemical formula $CF_2 = CF\text{-}CF_3$ and a T_g of 165 °C. Viton A-500 has a density ranging from 1780 to 1820 kg/m^3 and a T_g of −18 °C.[3] Bisphenol curing is used to polymerize the constituents.[2] An example of per- and polyfluoroalkyl substances (PFAS), these fluoroelastomers combine the advantages of fluoropolymers (excellent chemical and thermal resistance) and elastomers (good flexibility over a wide temperature range).[4] Several variants of Viton, A, B, and F, are based on fluorine content and molecular constituents. Viton A-500 consists of PVDF and HFP with a fluorine content of 66% [Fig. 1(a)], while Vitons B and F include tetrafluoroethylene (TFE) as a third constituent and have a fluorine content of 66%–70%.

The properties of this fluoroelastomer make it suitable as a binder material in plastic-bonded explosives (PBXs), which consist of explosive materials combined with a polymer binder.[5] In particular, the ease in processing due to Viton A's ductile nature makes it especially useful for mechanically sensitive or highly reactive explosives.[6] In addition, this fluoroelastomer A is used in the automotive and aerospace fields for gaskets, seals, and O-rings, where chemical resistance and a wide temperature range are paramount.[7] Since polymers can encounter high pressures and temperatures in these applications, a thorough understanding of their behavior under these conditions is required, particularly for Viton A, which has been less studied than Viton B.[8–11] It is also crucial to quantify and document the properties of these PFAS materials in the search for potential replacements[12] that will match and even exceed the performance of these fluoroelastomers in various applications.

Several static high-pressure studies of polymer binders have been reported. Stevens *et al.*[13] investigated Sylgard® 184, Estane® 5703, and poly(ethylene-vinyl acetate vinyl alcohol) (VCE) using Brillouin scattering in diamond anvil cells (DACs) to obtain pressure dependencies of sound velocities, elastic constants, mechanical properties, and equation-of-state (EOS) parameters to 12 GPa. Stevens *et al.*[14] and Benjamin *et al.*[15] used the same techniques to examine the binder material Kel-F® 800 to 18.5 and 85 GPa, respectively. These experiments provided a better understanding of polymer behavior over a wide pressure range, demonstrating that a significant change in polymer behavior occurs under 2 GPa before leveling off at pressures above 2 GPa, which is attributed to the collapse of free volume within the polymer. Ahart and Hemley[16] found similar behavior utilizing the same techniques to determine the EOS of ballistic gelatin to 12 GPa. Dattelbaum *et al.*[17] used an alternate image analysis method of the cross-sectional area in a DAC to extend the static EOS of Sylgard 184 to 10 GPa. Jordan *et al.*[18] performed simultaneous ultrasonic and XRD *in situ* using a Paris–Edinburgh (PE) press to obtain pressure dependencies of sound velocities, elastic properties, and density and examined the structure evolution for several polyethylene variants. Similar studies were conducted on polyurea crystals.[19]

Dynamic compression experiments have also been conducted on these polymer binders. Shock Hugoniot measurements on Viton B by Millett *et al.*[20] revealed a linear shock velocity–particle velocity relationship higher than that measured for PVDF and polytetrafluoroethylene (PTFE), indicating a stiffer material. A more recent shock study by Millett *et al.*[8] revisited Viton B to investigate the behavior of shear strength behind the shock front and to compare it to tetrafluoroethylene–hexafluoropropylene–vinylidene fluoride (THV 500), PVDF, and PTFE.[8] Dattelbaum *et al.*[21] conducted dilatometry measurements to 0.2 GPa and shock Hugoniot experiments to 10 GPa on THV-500 and fitted several EOS. Jordan *et al.*[18] measured high-density polyethylene (HDPE), which is

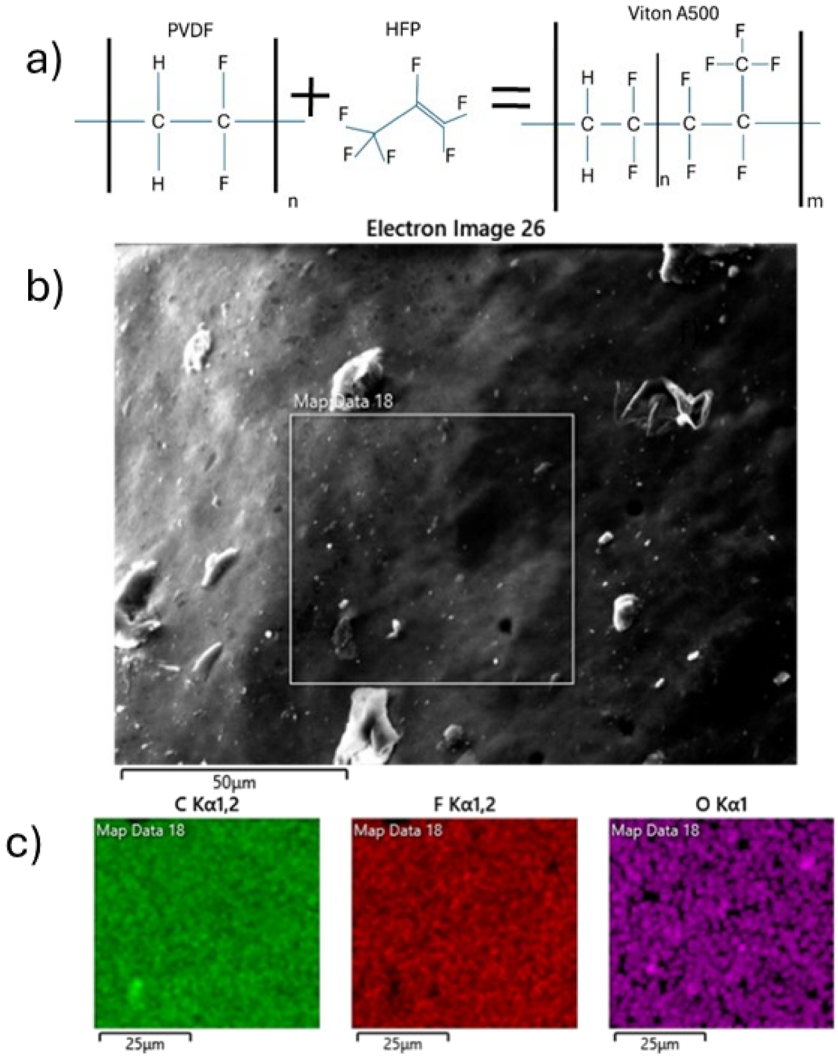

FIG. 1. (a) Chemical structure of the homopolymer, HFP, and the copolymer Viton A-500. (b) SEM image of the fluoroelastomer copolymer. (c) Elemental composition distribution of the fluoroelastomer, with green, red, and purple showing carbon, fluorine, and oxygen, respectively.

partially crystalline, to obtain the EOS and document phase transitions.[22] While Viton A has not been characterized at static high pressures, Viton B[9–11,20] and many related binder polymers[13–15] have elastic and mechanical properties reported to gigapascal pressures. In this study, we use the ultrasonic pulse-echo method with a PE press and Brillouin spectroscopy with DACs to determine the pressure dependencies of acoustic velocities, EOS, and elastic properties of Viton A-500 at room temperature.

Phasing out PFAS materials in favor of other polymers requires detailed knowledge of the physical and mechanical properties at relevant pressures. This study will attempt to match Viton A's desirable elastic and mechanical properties to non-PFAS polymers to suggest suitable replacements.

II. RESULTS AND DISCUSSION

A. Scanning electron microscopy (SEM) measurements

Energy-dispersive x-ray spectroscopy (EDXS) and field-emission scanning electron microscopy (FESEM) were used to confirm the composition and homogeneity of Viton. FESEM measurements were performed using an IT500HR SEM, and x-ray spectra were analyzed using the K-series of the constituents. All Viton A samples analyzed in this study were obtained from The Chemours Company.[2] Samples were prepared by cutting several 1–3 mm slices and mounting them on a sample stage. Height was pre-measured to allow for precise focus of electrons on the samples. As both samples produced clear images, sputtering was not required.

Several regions within the samples were analyzed to confirm consistent results. Averages of multiple readings were taken to quantify composition. Figure 1(b) shows representative SEM images, constituent concentration, and EDX spectra for this fluoroelastomer. Viton A displayed good homogeneity over nanometer-length scales, with carbon and fluorine distributed evenly [Fig. 1(c)], as shown by the intensity graphs. In addition, the Viton samples tested have regions where oxygen concentration was increased without fluorine. These intensities may correspond to hydrocarbon impurities introduced when preparing samples for SEM measurement. Several pieces of the fluoroelastomer were analyzed in multiple places, and there is approximately a 1:1 ratio of carbon to fluorine without substantial variation. Table I shows quantitative values for percentages of carbon and fluorine and their ratio in the Viton A sample, Viton. Trace elements were present but amounted to less than 1% of the composition. The trace elements are likely environmental contamination from sample handling and preparation.

TABLE I. Percentages of carbon, fluorine, and minor elements and carbon–fluorine ratio in Viton A.

Element	Composition (%)
Carbon (%)	49.8 ± 2.4
Fluorine (%)	49.6 ± 2.4
Minor elements	~1%
C/F	1.0 ± 0.1

B. Ultrasonic measurements

Ultrasonic, energy-dispersive x-ray diffraction (EDXD), and x-ray radiography measurements were performed to investigate the elastic properties of Viton A and develop an equation of state (EOS). The data were collected at the beamline 16BM-B (HPCAT) at the Advanced Photon Source (APS), Argonne National Laboratory (ANL). Detailed descriptions of the ultrasound velocity measurements at the beamline 16BM-B may be found in Ref. 23. A Paris–Edinburgh (PE) press was used to compress the sample [Fig. 2(a)]. The PE press has two opposing cupped tungsten carbide anvils between which a sample cell was placed. The sample cell consisted of concentric rings of MgO, boron epoxy, and Lexan surrounding the sample. An alumina buffer rod and a backing plate were used for acoustic coupling, and the flat-edge interfaces between the sample and the alumina were lined with Au foil (2 μm)) to provide contrast in radiography images. ZrO_2 caps were placed at the top and bottom of the sample cell. The sample was prepared by cutting and shaping a portion of the fluoroelastomer A into a cylinder with a height of 1 mm and a diameter of 1.5 mm before loading into the MgO ring of the sample cell. A 10-degree Y-cut $LiNbO_3$ transducer was used to generate and receive both compression and shear waves simultaneously.[23] Ultrasonic, radiographic, and XRD measurements were performed from 0.1 MPa to 5.65 GPa.

The ultrasound speeds at high pressures were measured using a variant of the pulse-echo technique.[24] The experimental setup consists of an ultrasonic transducer mounted to the top anvil of the PE press.[19] The ultrasound waves are generated by the transducer and propagate to the sample cell, and an oscilloscope records the waveforms of the ultrasound echoes reflected to the transducer. The interfaces in the sample cell that generate the reflected echoes are shown with blue arrows in Fig. 2(a). The primary reflections are R_0 from the top of the sample cell, R_1 from the top of the sample (sample-top), and R_2 from the bottom (sample-bottom). Figure 2(b) shows a representative sound wave from the fluoroelastomer of the longitudinal-acoustic (LA) and transverse-acoustic (TA) mode reflections. Each reflection is labeled with its corresponding interface in Fig. 2(a). Figure 2(c) shows LA-mode echoes ranging from 0.49 to 5.65 GPa, illustrating how sample echoes may be identified. R_2 is known to be from the sample due to its pressure dependence and is identified as the reflection from the bottom of the PEC. Naturally, the R_1 reflection must precede it. Upon identifying R_1 and R2, they may be selected for pulse-echo analysis to obtain LA-mode and TA-mode travel times. The ultrasonic pulse-echo technique was used with frequencies of 16–50 MHz in 2 MHz steps. The SonicPy program was used to perform the analysis, for which details may be found in Ref. 25. Thickness was measured by using x-ray radiography to image the side view of the PE sample cell [Fig. 2(d)]. SonicPy[25] was used to determine the positions of the top [Fig. 2(e)] and bottom [Fig. 2(f)] gold foils and the average sample thickness.

Sample thickness and time-of-flight data were used to calculate the LA- and TA-mode velocities by

$$v_{LA} = \frac{2d}{\tau_{LA}}, \tag{1}$$

$$v_{TA} = \frac{2d}{\tau_{TA}}. \tag{2}$$

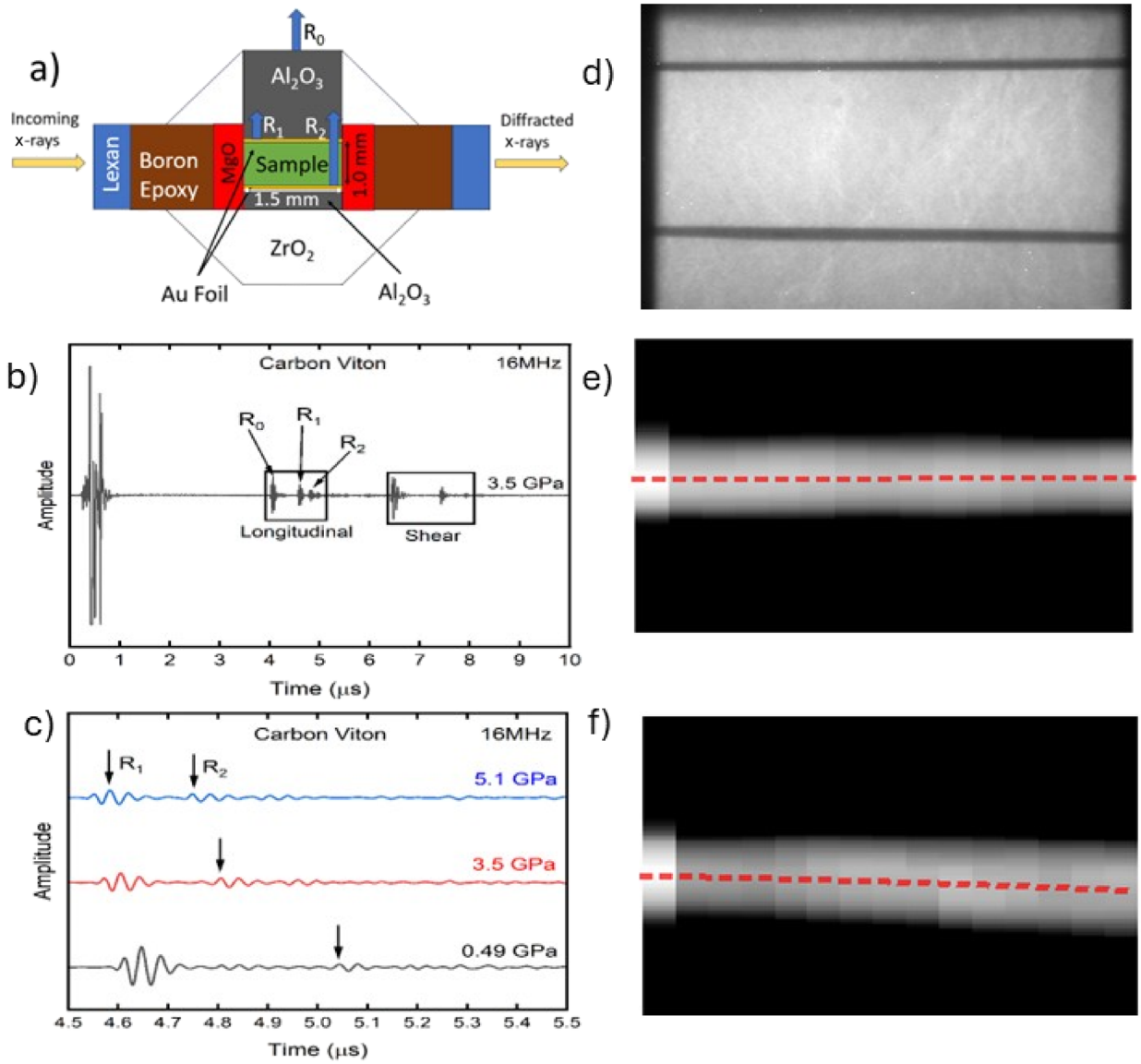

FIG. 2. Schematic of the key elements of a Paris–Edinburgh (PE) press and ultrasonic and radiography data measured therefrom. (a) Diagram of the PE press sample holder, adapted from Ref. 23. Ultrasonic reflections are labeled with blue arrows. Incoming and diffracted x rays pass through the Lexan/boron epoxy ring. The sample (green) is lined with Au foil. MgO used for pressure determination (purple) surrounds the sample. Zirconium oxide caps contain the fluoroelastomer sample. (b) Longitudinal-acoustic (LA) and transverse-acoustic (TA or shear) echoes in the fluoroelastomer at 3.5 GPa. Respective reflections in the PE press are labeled on the sound wave. (c) Pressure dependence of R_2 (sample bottom), observed shifting toward R_1 (sample top) as pressure increases from 0.5 to 5.1 GPa. Sample echoes are found by inspecting such pressure-dependent echoes. (d) Radiography image of the fluoroelastomer at 2.3 GPa showing the contrasting Au foil lines. (e) The top edge of the sample has a red dashed line showing the fit to the edge. (f) The bottom edge of the sample has a red dashed line showing the fit to the edge.

Pressure was estimated using the unit cell volumes of the surrounding MgO, obtained with *in situ* x-ray diffraction, and the MgO EOS from Kono *et al.*[26] PE press pressure was remotely controlled using a computer-controlled hydraulic syringe pump system. Velocities were obtained between 2.7 and 5.7 GPa. Further discussion of the data is provided in the supplementary material.

C. Brillouin spectroscopy

Brillouin spectroscopy was used to measure lower-pressure data to supplement ultrasonic measurements. Symmetric-type diamond anvil cells (DACs) were used with type IIa diamonds and 500 μm culets. Measurements were carried out in a symmetric scattering geometry [Fig. 3(a)] with a 532 nm exciting laser using a tandem

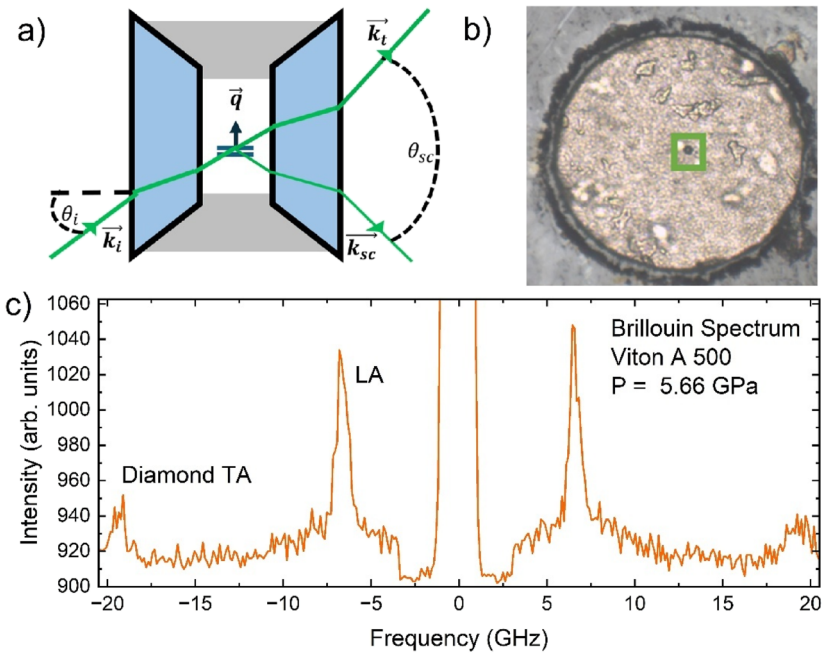

FIG. 3. (a) Schematic of Brillouin scattering spectroscopy in the symmetric scattering geometry. (b) View of a Viton A sample loaded in a DAC with a rhenium gasket and ruby pressure marker (within the green square). (c) Representative Brillouin spectrum of the fluoroelastomer, showing the inelastic diamond TA and Viton® A LA modes and the elastic Rayleigh peak.

Fabry–Pérot interferometer. Mirror spacings were changed between 7 and 13 mm to resolve lower and higher frequency regions, corresponding to a scanning range of 52.33 to 28.18 GHz and a finesse between 80 and 120.[27] Figure 3(b) shows a top-down view of the gasket hole containing the Vion A sample and a green box highlighting a ball ruby, whose fluorescence was used as the pressure gauge.[28,29]

Brillouin spectroscopy measures the intrinsic properties of a material at the gigahertz frequency range as opposed to ultrasonic spectroscopy's megahertz range. The fundamental principle behind Brillouin spectroscopy for disordered materials is the inelastic scattering of light: An incident laser impinges on the material, providing the energy requisite for density fluctuations. This fluctuation inelastically scatters light, whose frequency shift is proportional to the acoustic velocity of the sample [Fig. 3(c)].

The Brillouin frequency shift, $\Delta\nu$, is measured with an excitation laser with a wavelength λ_l, which imparts a transfer momentum $\vec{k_{sc}} = \vec{k_i} + \vec{q}$, at an angle θ. The symmetric scattering geometry accounts for the index of refraction by utilizing Snell's law, $n_{Viton} \sin\left(\frac{\theta}{2}\right) = \sin\left(\frac{\theta_{sc}}{2}\right)$, removing the necessity of prior knowledge of the index of refraction,

$$\Delta\nu = 2vk \sin\left(\frac{\theta}{2}\right) = \frac{2v}{\lambda_l} n_{Viton} \sin\left(\frac{\theta}{2}\right) = \frac{2v \sin\left(\frac{\theta_{sc}}{2}\right)}{\lambda_l}, \quad (3)$$

which in turn provides the equations for the longitudinal and transverse velocities,

$$v = \frac{\lambda_l \Delta\nu_{sym}}{2 \sin\left(\frac{\theta_{sc}}{2}\right)}. \quad (4)$$

One challenge in interpreting Brillouin scattering results is the possibility of frequency dispersion compared to the MHz-regime ultrasonic spectroscopy. Such frequency dispersion effects may indicate that the high-frequency Brillouin data appear stiffer than lower-frequency ultrasonic data for very soft materials.[13–16,30] This difference leads Brillouin data to give a higher bulk modulus (K_0) value compared to that obtained by ultrasonic spectroscopy.[13]

D. Acoustic velocities

LA- and TA-modes measured by ultrasonic and Brillouin spectroscopy indicate a smooth increase as a function of pressure, with the measurements from both spectroscopic techniques in agreement, including the region of overlap (Fig. 4). As is typical for polymers, the acoustic velocities of Viton A increase more rapidly at low pressures and slowly level off at higher pressures. The initial steep increase in the LA velocity arises from the polymer's free volume collapse during initial compression.[17,31] In the PEC ultrasonic measurements, pressure was unreliable below ~2.5 GPa due to the MgO ring used for pressure calibration [Fig. 2(a)] not being fully compacted. The measured MgO strain reflected a slower pressure increase than expected. A brief discussion of our choice to truncate our data at ~2.7 GPa is provided in the supplementary material. Ultrasonic LA- and TA-signals were present below 2.7 GPa. However, acoustic coupling between each interface in the sample holder (Fig. 3) does not become robust until ~1 GPa due to insufficient contact between the interfaces. The absence of TA-mode velocities in polymers at low pressures arises from the inability of polymers to sustain transverse waves (at these frequencies) as pressures approach ambient conditions. The bulk velocity (v_B) was obtained from longitudinal (v_{LA}) and transverse (v_{TA}) velocities using

$$v_B^2 = v_L^2 - \frac{4}{3} v_T^2. \quad (5)$$

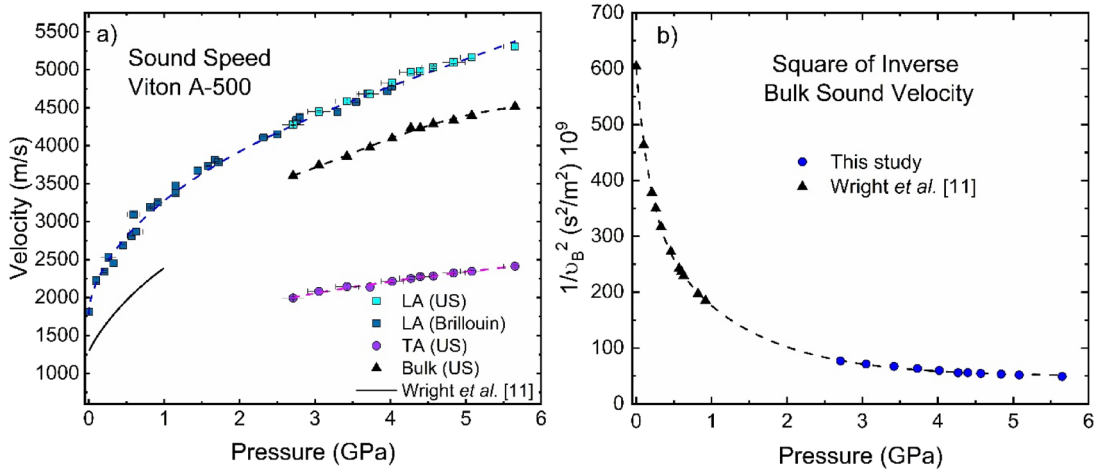

FIG. 4. (a) LA- and TA- and bulk velocities of the fluoroelastomer A collected with Brillouin and ultrasonic spectroscopy and low-pressure bulk measurements from Wright and Zoller.[11] The dashed lines are a guide for the eyes. (b) Inverse square velocity used for integration with Eq. (7). The dashed line is a guide for the eyes.

The low-pressure (<1 GPa) data used in the density calculation came from using Eq. (6) with dilatometry data obtained in previous studies.[9–11] Brillouin acoustic velocities were used to complement the ultrasonic data in our analysis of the elastic properties of the material,

$$\frac{1}{v^2} = \left(\frac{\partial \rho}{\partial P}\right)_S. \tag{6}$$

E. Pressure–density relations

Density–pressure relationships for Viton A were obtained using the following equation:

$$\rho - \rho_o = \int_{P_o}^{P} dP \frac{\gamma}{v_B^2} \cong \sum_{i=1}^{N} \frac{1}{2}\left(\frac{1}{v_{B,i}^2} + \frac{1}{v_{B,i+1}^2}\right)\Delta P_i, \tag{7}$$

where ρ_0 and ρ are the initial and current density, P_0 and P are the initial and current pressure, v_B is the bulk velocity, and γ is c_p/c_v, the ratio of constant-pressure to constant-volume specific heat. γ was taken to be 1, since $\gamma \approx 1$ for solid materials.[32] An initial density of 1820 kg/m^3 was used for calculations as specified by the Viton A datasheet.[2] The integrand [Fig. 4(b)], $1/v_B^2$, shows a rapid increase at low pressures, corresponding to free-volume collapse. Likewise, the free volume collapse is also seen with the rapid increase in density at low pressures, which is pictured in the inset of Fig. 5(a). At

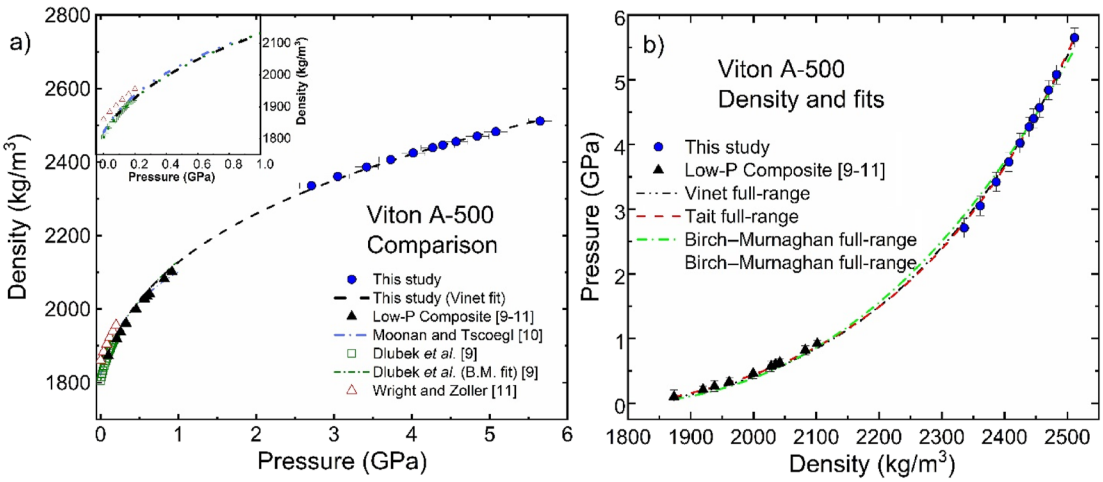

FIG. 5. (a) Comparison of the fluoroelastomer ρ–P data in this study with several experiments[9–11] carried out at lower pressures. (b) Density–pressure relation was determined from the acoustic velocities and Vinet, Birch–Murnaghan, and Tait EOS fits. Tait, Birch–Murnaghan, and Vinet EOS fit parameters are listed in Table II.

higher pressures, density changes significantly less with pressure, as is typical of materials not undergoing a phase transition. The gap in data between 1.0 and 2.7 GPa is caused by well-known experimental limitations in obtaining acoustic velocity or density for rubbery polymers in this pressure range.[9–11,13] We discuss the effects of the gap on the integration error in the supplementary material.

F. Equation of state analysis

Several EOS were fit to the density–pressure data and compared with previously examined amorphous binders (Fig. 5). The Vinet, Birch–Murnaghan, and Tait EOS are broadly used in materials science for highly compressible materials.[33–36] The Vinet equation of state is a semi-empirical function that uses relative linear strain relative to the ambient volume V_0, $x = \left(\frac{V}{V_0}\right)^{\frac{1}{3}}$, ambient bulk modulus ($K_0$), and its pressure derivative (K_0'). The Vinet EOS is derived from a postulated universal energy function for solid crystalline materials[35] discussed further by Cohen *et al.*,[33]

$$P = 3K_0\frac{(1-x)}{x^2}\exp\left(\frac{3}{2}\left(K_0'-1\right)(1-x)\right). \tag{8}$$

From the Vinet EOS, the bulk modulus, defined as $K = -V\left(\frac{\partial P}{\partial V}\right)_T$, may also be written as

$$K(x) = \frac{K_0}{x^2}\left(2+(\eta-1)x-\eta x^2\right)\exp\left(\eta(1-x)\right), \tag{9}$$

where $\eta = \frac{3}{2}(K_0'-1)$.

The Birch–Murnaghan EOS is another commonly used P–V EOS in high-pressure studies. Based on a series expansion of the Eulerian strain,[33] it is written to the third order as

$$P = \frac{3}{2}K_0\left(x^{-7}-x^{-5}\right)\left(1+\frac{3}{4}\left(K_0'-4\right)\left(x^{-2}-1\right)\right). \tag{10}$$

The Tait EOS fits the initial density and bulk modulus, similar to the Vinet and Birch–Murnaghan EOS, but also includes a material-specific parameter n,

$$P = \frac{K_0}{n}\left(x^{-n}-1\right). \tag{11}$$

TABLE II. Vinet, Birch–Murnaghan, and Tait EOS parameters for this fluoroelastomer (K_0 is in unit of GPa).

EOS	Low pressures (<1 GPa)	High pressures (>2 GPa)	All pressures (0.1 MPa to 5.5 GPa)
Vinet	$K_0 = 2.9 \pm 0.02$ $K_0' = 11.1 \pm 0.03$	$K_0 = 2.0 \pm 0.03$ $K_0' = 14.3 \pm 0.1$	$K_0 = 2.4 \pm 0.3$ $K_0' = 12.9 \pm 0.3$
B.M	$K_0 = 2.8 \pm 0.02$ $K_0' = 13.6 \pm 0.1$	Fit did not converge	$K_0 = 1.4 \pm 0.3$ $K_0' = 34 \pm 9$
Tait	$K_0 = 3.1 \pm 0.01$	$K_0 = 2.8 \pm 0.05$	$K_0 = 3.0 \pm 0.1$

This empirical EOS was originally developed for use in liquids under pressure. The high compressibility of polymers makes this EOS useful. Table II shows K_0 and K_0' obtained from fitting Vinet, Birch–Murnaghan, and Tait EOS in the lower (0.1 MPa to 1 GPa) and higher (1–6 GPa) pressure ranges.

G. Comparisons with other binder polymers

Table III compares the EOS parameters to those of the other amorphous polymers, namely Estane 5703, VCE, Sylgard 184,[13] and Kel-F-800.[14] Viton A behaves somewhat stiffer than VCE, Sylgard 184, and Estane 5703, with a $K_0 \sim 2.9$ GPa, and has a low-pressure K_0 similar to that reported for Kel-F 800 by Stevens *et al.*[14] but much softer than the full-range EOS reported by Stevens *et al.*[14] In the case of the Kel-F EOS of Stevens *et al.*[14] and the Vinet fit for the fluoroelastomer A, Viton A displays both a softer K_0 and more compressible K_0'.[37] The similarity between the K_0 parameters in the low-pressure and full-range EOS indicates that the whole compression mechanism can be accounted for in the Tait and Vinet EOS. While the Birch–Murnaghan equation of state resembles the low-pressure modulus measured by the Tait and Vinet EOS, it does not converge at higher pressures. The Birch–Murnaghan equation of state is less suited to fit very compressible materials,[33] so its difficulty in fitting ambient-pressure modulus data is not too surprising.

Viton A shows a similar trend to the other binder polymers analyzed, indicating a mildly lower velocity relative to VCE, Sylgard 184, and Estane 5703, but quite similar to Kel-F [Fig. 6(a)]. Kel-F, however, has a measured TA-mode down to ambient

TABLE III. Comparison of the EOS of this fluoroelastomer with other polymers, namely Kel-F-800, Estane 5703, VCE, and Sylgard 184, separated into different pressure regimes (K_0 is in unit of GPa).

	Low pressures (<1 GPa)		High pressures (>2 GPa)		All pressures		
Material	K_0 (GPa)	K_0'	K_0 (GPa)	K_0'	K_0 (GPa)	K_0'	Reference
Viton A	2.9 ± 0.01	11.1 ± 0.03	2.0 ± 0.03	14.3	2.4 ± 0.3	12.9 ± 0.1	This work
Kel-F 800	2.8 (Brillouin)	30.6 (Brillouin)	N/A	N/A	7.5	10.0	14
(5.5 < P < 18.5 GPa)	2.0 (dilatometry)	30.0 (dilatometry)					
Kel-F 800[14]							
(to 85 GPa, LP < 5 GPa)	14.6 ± 1.0	8.0 ± 0.7	29.4 ± 1.1	7.2 ± 0.1	23.0 ± 0.8	6.5 ± 0.1	15
Estane 5703	N/A	N/A	N/A	N/A	2.84	17.1	
VCE	N/A	N/A	N/A	N/A	2.05	10.0	13
Sylgard 184	N/A	N/A	N/A	N/A	1.13	9.0	

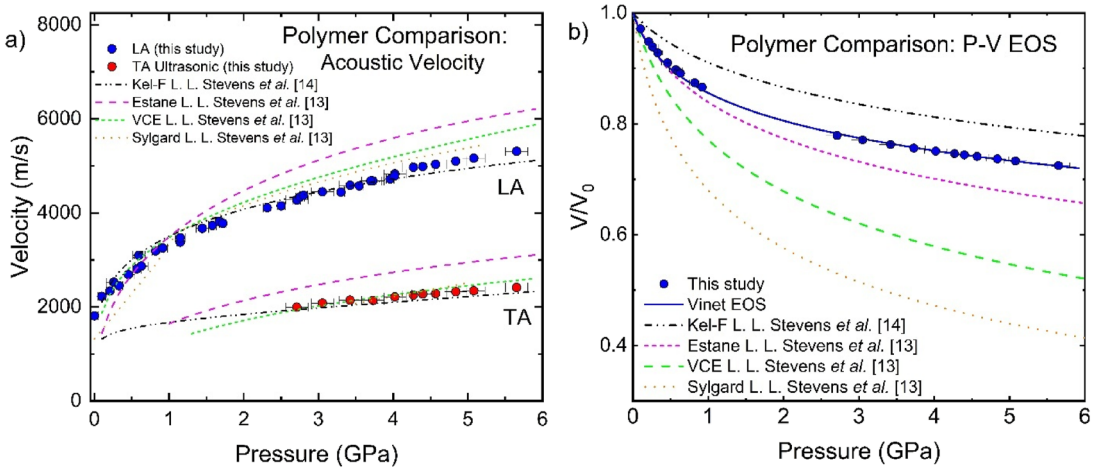

FIG. 6. (a) Comparison of the acoustic velocity of the fluoroelastomer and related binder polymers. Low-pressure fitting differences between polymers stem from the fewer and more scattered low-pressure data in Stevens *et al.*[13] (b) Comparison of the normalized P–V EOS of this fluoroelastomer and related polymers.

pressure on account of its high glass transition temperature (T_g = 28 °C), lending the ability for its internal structure to carry TA-modes at much lower pressures compared to Viton A (T_g = −18 °C). This observation is more clearly seen in the P–V EOS for these polymers [Fig. 6(b)], which indicates closer agreement of Kel-F and Viton A as less-compressible polymers relative to the three other binder polymers. Kel-F has a noticeably stiffer bulk modulus than Viton A and other bulk moduli in this study (Table IV). However, Viton A indicates a more similar modulus to Estane 5703 than Kel-F.

Several low-pressure experiments on this fluoroelastomer have measured P–V–T data. Their bulk moduli are presented in Table IV. Wright and Zoller[11] and Dlubek *et al.*[9] used dilatometry measurements to obtain P–V–T data. Moonan and Tschoegl[10] obtained the pressure dependence of the volume using an extensometer. These three studies relied on mechanical, rather than scattering, techniques to determine the P–V–T data. These data obtained with direct measurement indicate a lower bulk modulus on average. These are compared with the Kel-F data, showing Brillouin scattering obtaining a low-pressure K_0 of 2.8 GPa, compared with the dilatometry-measured 2.0 GPa. The exception to this is Millet's study,[20] which looks at Viton B under dynamic compression conditions,[19] and Wright *et al.*,[11] which uses a different EOS to fit their measured data, possibly contributing to the apparent difference.

III. ELASTICITY AND CAUCHY-LIKE RELATIONS

The elastic constants are related to longitudinal and transverse velocities and densities using the following relations:

$$c_{11} = M_S = \rho v_L^2, \tag{12}$$

TABLE IV. Bulk moduli of Viton using different experimental techniques for measurement.

Sample	K_0 (GPa)	Probe type	Source
Viton A-500	2.4 (P < 1 GPa 2.0 (P > 2.5 GPa)	Brillouin+Wright *et al.*	This study
Viton A	1.8	Dilatometry	Fluoroelastomer handbook[38]
Viton	0.27 2.8 (Vinet EOS)	Dilatometry	Wright and Zoller[11]
Viton B	4.4	Shock data + TVH-500 extrapolation	Millet *et al.*[8]
Viton B	2.0	Extensometer	Moonan and Tschoegl[10]
PVDF–HFP	1.7	Dilatometry	Dlubek[9]
Kel-F 800	7.5 (0–18 GPa 2.8 (P < 2 GPa) 2.0 (P < 2 GPa) 8.0	Brillouin Brillouin Dilatometer Brillouin	Stevens *et al.*[14] Benjamin *et al.*[15]

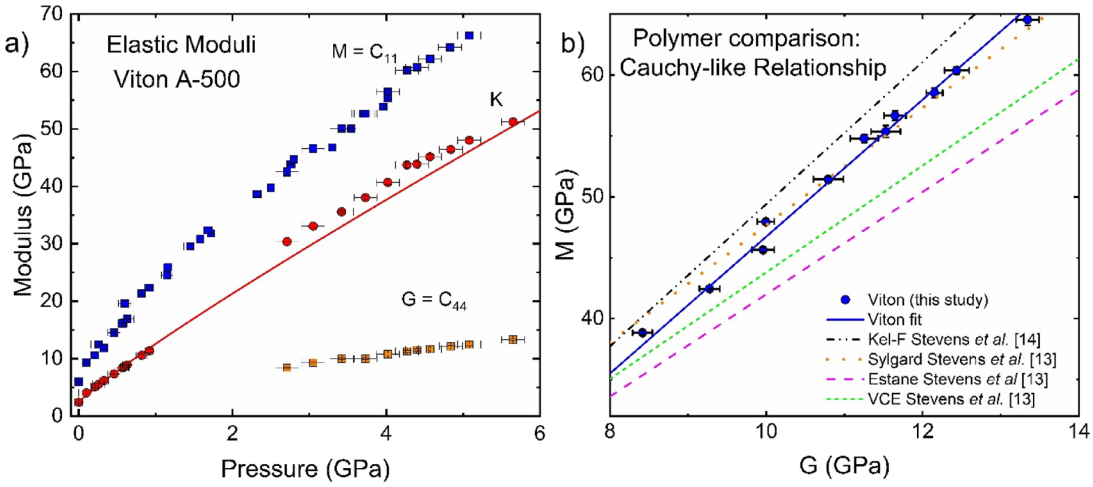

FIG. 7. (a) Pressure dependence on the bulk modulus (K_S), the longitudinal modulus (M_S), and the shear modulus (G_S). The pink circle at the origin reflects the zero-pressure bulk modulus determined by the Vinet EOS. The red solid line shows the bulk modulus determined from Eq. (9). Low- and high-pressure modulus fits were done to account for the 1.5 GPa gap. (b) Cauchy-like relationship for this fluoroelastomer and similar polymers.

$$c_{44} = \frac{c_{11} - c_{12}}{2} = G_S = \rho v_T^2, \tag{13}$$

$$K_S = \rho v_B^2, \tag{14}$$

where c_{11}, c_{12}, and c_{44} are elastic constants; M_S, G_S, and K_S are the longitudinal, shear, and bulk moduli, respectively (at constant entropy S); and v_L, v_T, and v_B are the longitudinal, transverse, and bulk velocities, respectively.

Figure 7(a) shows the pressure dependence of the longitudinal and shear moduli. Like other polymers, this fluoroelastomer exhibits a significant increase in elastic moduli under pressure: M_S ranges from about 7 to 70 GPa and K_S increases from 2 to 50 GPa. G_S exhibits far less pressure dependence, adopting a more linear dependence with values from 1 to 15 GPa (Table V). Our Viton A modulus data indicate higher pressure derivatives. We believe that this stems from the rapid densification evident in Fig. 6(b). We also determined the Cauchy-like relation [Fig. 7(b)] with our modulus data,

$$M_S = A + BG, \tag{15}$$

where M_S is the longitudinal modulus given by $M = \rho v_L^2$, G is the shear modulus given by $G_S = \rho v_T^2$, and A and B are fitting parameters. When $B = 3$, the effective intermolecular interactions of the material can be modeled with a central potential.[39] Table VI shows the B parameter for Viton A compared to values obtained for VCE and Estane®. Viton A's B value is 5.62, which indicates that its effective intermolecular interactions deviate from a central potential. The B values are closer to those of Kel-F (B = 5.86) than to Estane (B = 4.2).

TABLE V. Pressure derivatives of elastic moduli.

Material	$\partial M_S/\partial P$	$\partial K_S/\partial P$	$\partial G_S/\partial P$	Source
Viton A	14.7 ± 0.5	9.4 ± 0.2	4.1 ± 0.2	This study
VCE	8.3	5.6	1.9	8
Sylgard 184	8.5	5.6	1.6	8
Estane 5703	8.5	5.8	1.9	8

TABLE VI. Cauchy-like parameters.

Polymer	B-parameter	Source
Viton A	5.6	This study
Kel-F 800	5.8	Stevens *et al.*[13]
Estane 5703	4.4	Stevens *et al.*[13]
VCE	3.5	Stevens *et al.*[13]
HDPE	3.4	Jordan *et al.*[18]

IV. POISSON'S RATIO

The Poisson's ratio (PR) for the fluoroelastomer was determined and compared to common materials and other polymers (Fig. 8). The PR is found from the longitudinal and transverse velocities using

$$\sigma = \frac{v_L^2 - 2v_T^2}{2(v_L^2 - v_T^2)}. \tag{16}$$

At low pressures, the PR for the fluoroelastomer is more similar to ideal liquids and polymers and nearly matches the low-pressure literature value of Estane.[40] At high pressures, the PR data for the fluoroelastomer are close to those of the other binder polymers: Sylgard 184, VCE, and Estane 5703.[13] The data fall between 0.3 and 0.4, which indicates the similar behavior of the polymers under pressure. The high-pressure agreement of all polymers with the PR

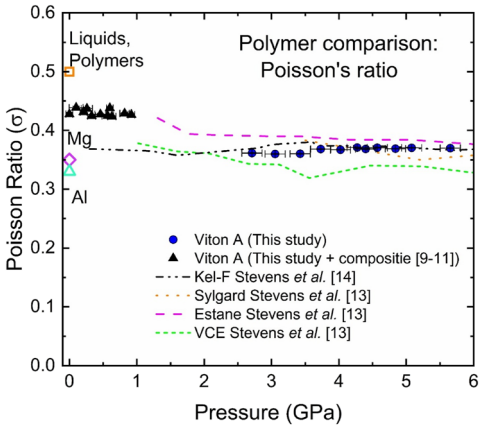

FIG. 8. Poisson's ratio data for the fluoroelastomer compared to other polymers (VCE and Estane 5703) and metals (Al and Mg shown as a green triangle and purple diamond, respectively). The orange square indicates the Poisson's ratio expected for polymers and liquids that cannot support transverse modes. The low-pressure data from this study are a composite of several dilatometry measurements used to calculate υ_B with Eq. (5), which, through Eq. (6), obtains υ_T used in Eq. (16).

seen in metals is significant. This fluoroelastomer shows weak semi-crystallinity (discussed in the supplementary material), while the other polymers are amorphous. Suppose that the semi-crystalline portion of the fluoroelastomer is not substantial to its elastic properties. In that case, the bulk properties of this fluoroelastomer will reflect those of amorphous materials, as the PR data show. In addition, the 0.3–0.4 range of values is like those found for metals at ambient pressure, indicating that the polymers under compression behave similarly to metals. This could result from the collapse of free volume within the polymers, which reduces the degrees of freedom that atomic chains can adjust and forces them closer together, making the structure of the polymers closely packed and more like a crystalline material. This has implications for the equation of state; there are clearly two pressure regimes where the longitudinal and shear velocities relate to each other differently—fluid-like at low pressures and metal-like at high pressures.

V. CONCLUSIONS

We have measured the acoustic velocities of Viton A-500 using both ultrasonic and Brillouin spectroscopies to obtain a wide-range EOS from 0.1 MPa to 5.5 GPa. Transverse-mode velocities were only measured with ultrasonic spectroscopy due to instrumental limitations, a weak elasto-optic constant, and the inability to sustain transverse waves at low pressures. The Tait, Birch–Murnaghan, and Vinet EOS were fit to the ρ–P data obtained from the acoustic velocities over the whole pressure range, and at lower (<2 GPa) and higher pressures (>2 GPa). We see an agreement between the lower-pressure data and the full-range equations of state, indicating a smoother pressure increase than Kel-F. The fluoroelastomer's bulk, shear, and longitudinal moduli, the modulus pressure derivatives, Poisson's ratio, and Cauchy-like parameters were calculated using the measured acoustic velocity and density data. Compared to the data reported for VCE, Estane 5703, Sylgard 184, and Kel-F, the results indicate that this fluoroelastomer is a stiffer material than VCE, Estane, and Sylgard but softer than Kel-F. Overall, Estane 5703 shows the closest similarity to this fluoroelastomer. The Cauchy-like parameter is more like Kel-F than the non-fluoroelastomers. The Poisson's ratio of Viton remains close to 0.33 as a function of pressure in the post-volume collapse region, similar to that of metals under ambient conditions. These analyses and comparisons should aid the search for non-PFAS materials having similar EOS, elasticity, and other properties for future applications.

SUPPLEMENTARY MATERIAL

See the supplementary material for an overview of the ultrasonic experimental analysis, a discussion regarding pressure determination using the MgO EOS in a PE press, a discussion about alignment effects on Brillouin scattering velocity, the pressure–velocity data table used for this study, and a discussion about the integration error due to the gap between 1 and 2.7 GPa in the EOS data.

ACKNOWLEDGMENTS

This work was supported by Extreme EnErgy Density (EXEED), an Army HBCU/MI Center of Excellence at the University of Illinois Chicago, under Grant No. W911NF2110275 from the Army Research Office; by the U.S. Department of Energy-National Nuclear Security Administration (DOE-NNSA) cooperative agreement DE-NA-0004153 (Chicago/DOE Alliance Center, CDAC); and by the DOE Office of Science, Fusion Energy Sciences (Grant No. DE-SC0020340). Ultrasonic and synchrotron x-ray experiments were performed at HPCAT (Sector 16) Advanced Photon Source (APS), Argonne National Laboratory (ANL). HPCAT operations are supported by DOE-NNSA's Office of Experimental Sciences. APS is a DOE Office of Science User Facility operated for the DOE Office of Science by ANL under Contract No. DE-AC02-06CH11357.

AUTHOR DECLARATIONS

Conflict of Interest

The authors have no conflicts to disclose.

Author Contributions

C.M.Z. and J.S. contributed equally to this work.

Charlie M. Zoller: Data curation (lead); Formal analysis (lead); Investigation (lead); Visualization (lead); Writing – original draft (lead); Writing – review & editing (lead). **Jonathan Simon**: Data curation (lead); Formal analysis (lead); Investigation (lead); Writing – original draft (lead). **Rostislav Hrubiak**: Methodology (supporting); Resources (supporting); Software (supporting); Writing – review & editing (equal). **Curtis Kenney-Benson**: Methodology (supporting); Writing – review & editing (equal). **Stephen A. Gramsch**: Funding acquisition (equal); Project administration (equal); Writing – review & editing (equal). **Dana M. Dattelbaum**: Conceptualization (lead); Funding acquisition (equal); Project administration (equal); Writing – review & editing (equal). **Muhtar**

Ahart: Formal analysis (equal); Investigation (equal); Methodology (equal); Supervision (lead); Writing – review & editing (equal). **Russell J. Hemley**: Conceptualization (lead); Funding acquisition (equal); Project administration (equal); Supervision (equal); Writing – review & editing (equal).

DATA AVAILABILITY

The data that support the findings of this study are available within the article and its supplementary material.

REFERENCES

[1] Y. Wang and Y. Bai, "The functionalization of fluoroelastomers: Approaches, properties, and applications," RSC Adv. **6**, 53730–53748 (2016).

[2] *Viton A-500 Fluoroelastomers* (Chemours Company FC, 2016).

[3] Q.-L. Yan, S. Zeman, and A. Elbeih, "Thermal behavior and decomposition kinetics of Viton A bonded explosives containing attractive cyclic nitramines," Thermochim. Acta **562**, 56–64 (2013).

[4] R. E. Banks, B. E. Smart, and J. C. Tatlow, *Organofluorine Chemistry : Principles and Commercial Applications*, 1st ed. (Plenum Press, New York, NY, 1994).

[5] D. M. Hoffman, "Dynamic mechanical signatures of Viton A and plastic bonded explosives based on this polymer," Polym. Eng. Sci. **43**, 139–156 (2004).

[6] B. W. Asay, *Shock Wave Science and Technology Reference Library. Volume 5, Non-shock Initiation of Explosives* (Springer, Heidelberg, 2010).

[7] S. H. Lee, S. S. Yoo, D. E. Kim, B. S. Kang, and H. E. Kim, "Accelerated wear test of FKM elastomer for life prediction of seals," Polym. Test. **31**, 993–1000 (2012).

[8] J. C. F. Millett, E. N. Brown, N. K. Bourne, G. Whiteman, and G. T. Gray, "The shock induced mechanical response of the fluorinated tri-polymer, Viton B," J. Dyn. Behav. Mater. **7**, 436–446 (2021).

[9] G. Dlubek, J. Wawryszczuk, J. Pionteck, T. Goworek, H. Kaspar, and K. H. Lochhaas, "High-pressure dependence of the free volume in fluoroelastomers from positron lifetime and PVT experiments," Macromolecules **38**, 429–437 (2005).

[10] W. K. Moonan and N. W. Tschoegl, "Effect of pressure on the mechanical properties of polymers. 2. Expansivity and compressibility measurements," Macromolecules **16**, 55–59 (1983).

[11] G. P. Wright and P. Zoller, "Thermophysical properties of O-ring elastomers at pressures to 200 MPA," High Pressure Res. **3**, 282–284 (1990).

[12] M. Ateia and M. Scheringer, "From "forever chemicals" to fluorine-free alternatives," Science **385**, 256–258 (2024).

[13] L. L. Stevens, E. B. Orler, D. M. Dattelbaum, M. Ahart, and R. J. Hemley, "Brillouin-scattering determination of the acoustic properties and their pressure dependence for three polymeric elastomers," J. Chem. Phys. **127**, 104906 (2007).

[14] L. L. Stevens, D. M. Dattelbaum, M. Ahart, and R. J. Hemley, "High-pressure elastic properties of a fluorinated copolymer: Poly(chlorotrifluoroethylene-co-vinylidene fluoride) (Kel-F 800)," J. Appl. Phys. **112**, 023523 (2012).

[15] A. S. Benjamin, M. Ahart, S. A. Gramsch, L. L. Stevens, E. B. Orler, D. M. Dattelbaum, and R. J. Hemley, "Acoustic properties of Kel F-800 copolymer up to 85 GPa," J. Chem. Phys. **137**, 014514 (2012).

[16] M. Ahart and R. J. Hemley, "Sound velocity and equation of state of ballistic gelatin by Brillouin scattering," Materials **16**, 1279 (2023).

[17] D. M. Dattelbaum, J. D. Jensen, A. M. Schwendt, E. M. Kober, M. W. Lewis, and R. Menikoff, "A novel method for static equation-of state-development: Equation of state of a cross-linked poly(dimethylsiloxane) (PDMS) network to 10 GPa," J. Chem. Phys. **122**, 144903 (2005).

[18] J. L. Jordan, R. L. Rowland, J. Greenhall, E. K. Moss, R. C. Huber, E. C. Willis, R. Hrubiak, C. Kenney-Benson, B. Bartram, and B. T. Sturtevant, "Elastic properties of polyethylene from high pressure sound speed measurements," Polymer **212**, 123164 (2021).

[19] T. Eastmond, J. Hu, V. Alizadeh, R. Hrubiak, J. Oswald, A. Amirkhizi, and P. Peralta, "Probing high-pressure structural evolution in polyurea with in situ energy-dispersive x-ray diffraction and molecular dynamics simulations," Macromolecules **54**, 597–608 (2021).

[20] J. C. F. Millett, N. K. Bourne, and G. T. Gray III, "The equation of state of a fluorinated tripolymer," J. Appl. Phys. **96**, 5500–5504 (2004).

[21] D. M. Dattelbaum, S. A. Sheffield, D. Stahl, M. Weinberg, C. Kit Neel, and N. Thadhani, "Equation of state and high pressure properties of a fluorinated terpolymer: THV 500," J. Appl. Phys. **104**, 113525 (2008).

[22] D. Dattelbaum, B. Schilling, B. Clements, J. Jordan, C. Welch, and J. Stull, "Shock response and dynamic failure of high-density (HDPE) and ultra-high molecular weight polyethylene (UHMWPE)," J. Dyn. Behav. Mater. **2024**, 1–12.

[23] Y. Kono, C. Park, T. Sakamaki, C. Kenny-Benson, G. Shen, and Y. Wang, "Simultaneous structure and elastic wave velocity measurement of SiO_2 glass at high pressures and high temperatures in a Paris–Edinburgh cell," Rev. Sci. Instrum. **83**, 033905 (2012).

[24] C. Pantea, D. G. Rickel, A. Migliori, R. G. Leisure, J. Zhang, Y. Zhao, S. El-Khatib, and B. Li, "Digital ultrasonic pulse-echo overlap system and algorithm for unambiguous determination of pulse transit time," Rev. Sci. Instrum. **76**, 114902 (2005).

[25] R. Hrubiak and B. T. Sturtevant, "SonicPy: A suite of programs for ultrasound pulse-echo data acquisition and analysis," High Pressure Res. **43**, 23–39 (2023).

[26] Y. Kono, T. Irifune, Y. Higo, T. Inoue, and A. Barnhoorn, "*PVT* relation of MgO derived by simultaneous elastic wave velocity and in situ x-ray measurements: A new pressure scale for the mantle transition region," Phys. Earth Planet. Inter. **183**, 196–211 (2010).

[27] J. R. Sandercock, *Tandem Fabry–Perot Interferometer TFP-1 Operator Manual* (JRS Scientific Instruments, 2022).

[28] A. Dewaele, M. Torrent, P. Loubeyre, and M. Mezouar, "Compression curves of transition metals in the mbar range: Experiments and projector augmented-wave calculations," Phys. Rev. B **78**, 104102 (2008).

[29] H. K. Mao, J. Xu, and P. M. Bell, "Calibration of the ruby pressure gauge to 800 kbar under quasi-hydrostatic conditions," J. Geophys. Res. **91**, 4673, https://doi.org/10.1029/jb091ib05p04673 (1986).

[30] Y. Takagi, M. Ahart, T. Yano, and S. Kojima, "The liquid–glass transition in n-propanol: The pressure dependence of the Brillouin spectra," J. Phys.: Condens. Matter **9**, 6995 (1997).

[31] M. L. Williams, R. F. Landel, and J. D. Ferry, "The temperature dependence of relaxation mechanisms in amorphous polymers and other glass-forming liquids," J. Am. Chem. Soc. **77**, 3701–3707 (1955).

[32] S. Ayrinhac, "Heat capacity ratio in liquids at high pressure," J. Appl. Phys. **129**, 185903 (2021).

[33] R. E. Cohen, O. Gulseren, and R. J. Hemley, "Accuracy of equation-of-state formulations," Am. Miner. **85**, 338–344 (2000).

[34] E. J. Padilha Júnior, R. d. P. Soares, and N. S. M. Cardozo, "Analysis of equations of state for polymers," Polímeros **25**, 277–288 (2015).

[35] P. Vinet, J. H. Rose, J. Ferrante, and J. R. Smith, "Universal features of the equation of state of solids," J. Phys.: Condens. Matter **1**, 1941 (1989).

[36] F. Birch, "Equation of state and thermodynamic parameters of NaCl to 300 kbar in the high-temperature domain," J. Geophys. Res.: Solid Earth **91**, 4949–4954, https://doi.org/10.1029/jb091ib05p04949 (1986).

[37] R. Menikoff and T. D. Sewell, "Fitting forms for isothermal data," High Pressure Res. **21**, 121–138 (2001).

[38] R. T. Patil, *Vinylidene Fluoride Hexafluoropropylene Elastomers* (Oxford University Press, 1999).

[39] L. Elcoro and J. Etxebarria, "Common misconceptions about the dynamical theory of crystal lattices: Cauchy relations, lattice potentials and infinite crystals," Eur. J. Phys. **32**, 25–35 (2011).

[40] G. N. Greaves, A. L. Greer, R. S. Lakes, and T. Rouxel, "Poisson's ratio and modern materials," Nat. Mater. **10**, 823–837 (2011).